

Implications of Low Angle $\text{YBa}_2\text{Cu}_3\text{O}_{7-x}$ Bicrystal Transport Characteristics for Coated Conductor Applications

N. F. Heinig[†], G. A. Daniels, M. Feldmann, A. Polyanskii and D. C. Larbalestier

Applied Superconductivity Center, University of Madison-Wisconsin, Madison, WI
now at Lawrence Berkeley National Laboratory, Berkeley, CA

P. Arendt, and S. Foltyn

Los Alamos National Laboratory, Los Alamos, NM

Abstract—Coated conductor (CC) $\text{YBa}_2\text{Cu}_3\text{O}_{7-x}$ prototypes can now be made with critical current density, J_c (77K, 0T), values of 1 - 2 MA/cm² and full width half maximum (FWHM) in-plane misalignments of 7° - 15°. In order to understand better the current paths in such conductors, we have measured extended electric field - current density (E-J) characteristics in fields of 0 - 9 T at 77 K, comparing the data to that obtained on thin film bicrystals. We find that the E-J curves of the CC show little sign of weak coupling. We also investigate the role sample thickness plays in intergranular high field transport by measuring E-J curves up to 8 Tesla on 7°[001] tilt bicrystal films with thickness between 75 and 300 nm. We see that the intergrain irreversibility field increases with thickness, much as has been seen in single crystal samples. Magneto-optic imaging and scanning electron microscopy show that porosity in the $\text{YBa}_2\text{Cu}_3\text{O}_{7-x}$ layer and scratches in the ceramic buffer layers can also control J_c . These results show that the critical current density of coated conductors is limited on several length scales and by several different defect types.

I. INTRODUCTION

Coated conductors (CC) [1], [2], [3] are recently developed materials with some highly desirable properties for bulk-scale superconducting applications. Foremost of these properties is a very high critical current density, J_c , in large magnetic fields. Formed from biaxially textured $\text{YBa}_2\text{Cu}_3\text{O}_{7-x}$, the weak superconducting coupling seen at high angle grain boundaries [4], [5], [6], [7] that has limited bulk scale applications of $\text{YBa}_2\text{Cu}_3\text{O}_{7-x}$ is largely avoided. The challenge now is to scale-up the fabrication techniques so that long lengths of high J_c material can be made. In order to do so, understanding what is presently limiting the critical current density, J_c , would be very helpful. With critical current densities, J_c (77K, 0T), of 1 - 2 MA/cm², and a full width half maximum (FWHM) in-plane misalignment varying between 7° and 15°, it is clear that percolative current flow through low angle grain boundaries in these materials is to be expected. How much the critical current density is restricted by these low angle boundaries, and how much is due to other defects such as cracks, second phases, porosity, and highly misaligned regions is still very much an open question.

[†] Manuscript received Sept 15, 1998. This work was supported by the NSF MRSEC Program (DMR-9632427), the Electric Power Research Institute (RP8065-6) and AFOSR.

To address these issues, we compare CC prototypes fabricated at Los Alamos (LANL) using ion beam assisted deposition (IBAD) [1], [2], with $\text{YBa}_2\text{Cu}_3\text{O}_{7-x}$ single crystal and bicrystal films grown by pulsed laser deposition in Wisconsin. By comparing the microstructure and electromagnetic transport properties of the biaxially textured CC with those of individual low angle grain boundaries, we expect to understand how improving the CC texture can be expected to improve the total J_c of these materials.

This paper begins with a brief overview of the growth and processing of the CC and pulsed laser deposited (PLD) films, then continues with a comparison of high field current-voltage characteristics. The extended electric field - current density (E-J) curves were made in magnetic fields (H-llc) up to 9 Tesla at 77 K, and show that the CC materials behave much like single crystal films. There was also concern that different thickness' of these materials may affect the intergranular characteristics, so a study of $J_c(H)$ versus thickness of the PLD films is included and compared with the CC prototypes. We found that the high field inter- and intragrain J_c increased significantly with film thickness, as did the irreversibility field. To observe on what lengths scales the current is disrupted, magneto-optic imaging (MOI) and scanning electron microscopy (SEM) were used on both types of materials. These studies indicate that both porosity and highly misaligned grains can be barriers to supercurrent flow.

II. GROWTH AND PROCESSING

Two coated conductor samples were grown at LANL by pulsed laser deposition (PLD) directly onto a yttria-stabilized ZrO_2 (YSZ) layer. The first sample had the YSZ layer directly sputtered onto an Inconel-625 substrate by ion beam assisted deposition (IBAD). The textured $\text{YBa}_2\text{Cu}_3\text{O}_{7-x}$ layer was 0.90 μm thick and had an in-plane mosaic spread of 12.4° FWHM, as determined by phi scans of the [103] peak. The second sample was grown as above, except for a buffer layer of CeO_2 between the YSZ and the Inconel. This sample had an in-plane mosaic spread of 9.0°. Using a chemical etch, each sample was patterned with two transport links. The first sample contains link A and B, and the second link C and D.

C-axis oriented $\text{YBa}_2\text{Cu}_3\text{O}_{7-x}$ bicrystal films were made at the University of Wisconsin by PLD onto 7°[001] symmetric

tilt SrTiO₃ bicrystal substrates. They were grown using a KrF laser at 5.3 Hz with a pulse energy of 460 mJ in an atmosphere of 210 mTorr of oxygen. For all the films, the growth temperature was 840°C, as measured by an optical pyrometer reading outside the YBa₂Cu₃O_{7-x} plume. A constant temperature during growth was maintained by using the pyrometer readings to control the substrate heater. After growth, the films were patterned with photolithography and dry etched to make well-defined inter- and intragranular test links. Film thickness was calibrated by using an alpha-stepper, which has an approximate accuracy of 5%. Rocking curve scans of the [108] peak show a FWHM of less than 1°, indicating negligible in-plane mosaic spread.

III. ELECTROMAGNETIC PROPERTIES

The CC samples were patterned into bridges approximately 300 μm wide and 5mm long, with the long dimension parallel to the long dimension of the IBAD tape. Zero field J_c measurements in liquid nitrogen at Los Alamos (75K) found link A had $J_c = 0.70$ MA/cm², link B had $J_c = 1.30$ MA/cm², and link C had $J_c = 1.2$ MA/cm². Link D did not have a measurable J_c . Link A and B had J_c values that differed by almost a factor of 2, despite being positioned close together on the same sample. In addition, although the second sample containing link C had much better in-plane texture than the first sample (9.0° versus 12.4° FWHM), a corresponding increase in J_c was not seen.

To further understand these observations, extended voltage-current (V-I) characteristics were measured in magnetic fields of 4 to 9 Tesla at 77K, and compared to similar measurements on single crystal and bicrystal YBa₂Cu₃O_{7-x} films [7], [8]. These measurements were carried out in a variable temperature gas cryostat. The data from link A and B are shown in Fig. 1. Both link A and B behave similarly to a single crystal film, and both have an irreversibility field, H^* , at about 5.5 Tesla. As discussed earlier [7]-[9], these characteristics include a monotonic V-I curve that gradually changes curvature in increasing field, and on a log-log plot, approximately evenly spaced V-I curves with field, corresponding to an exponential decrease in J_c with magnetic field.

In the earlier bicrystal work [7], [8], signs that the grain boundary was beginning to restrict the supercurrent could be seen in the high field V-I curves. These signatures of grain boundary weak coupling included a V-I characteristic with a sigmoidal shape, and rather closely spaced V-I curves below H^* , corresponding to a "plateau" in J_c with field, which follows a very rapid decline in $J_c(H)$ between zero and one Tesla. A slight indication of these features is apparent when comparing link A to link B, but this evidence of weaker coupling in link A is notable mainly when considered in conjunction with the magneto-optic imaging results of the next section.

Much previous work on bicrystals has concentrated on thin

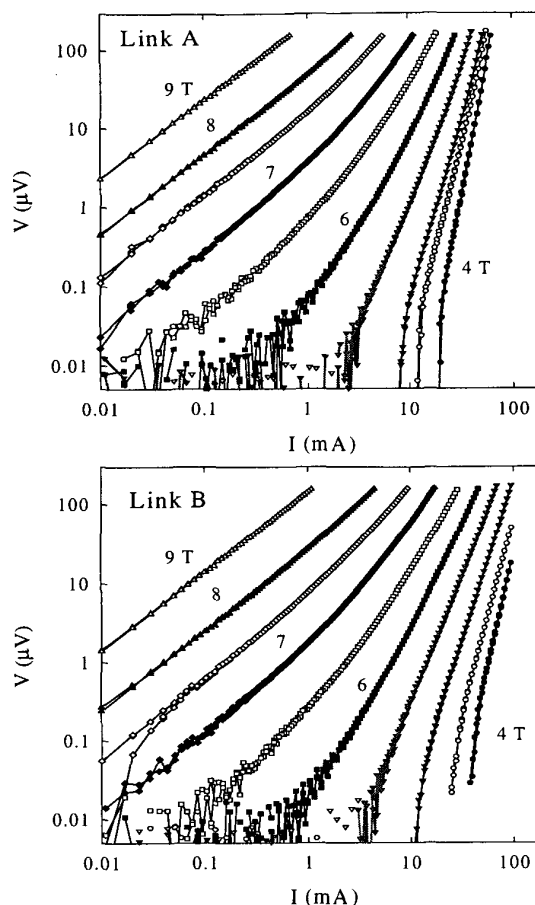


Fig. 1. Extended voltage-current curves in high perpendicular magnetic fields of 4 to 9 T at 77 K, for link A and link B of the first coated conductor sample. Link A had $J_c(0) = 0.7$ MA/cm², and link B had $J_c(0) = 1.3$ MA/cm².

films. Since the irreversibility field and other high field transport properties can depend on geometrical factors like film thickness [10], [11], the effect of film thickness on transport behavior was studied in three 7°[001] YBa₂Cu₃O_{7-x} bicrystals with thickness 0.075 μm, 0.15 μm and 0.3 μm. Great care was taken to ensure that all the films were grown at the same temperature. The intergrain and intragrain critical current density ratio J_n/J_c was measured in zero field at 77 K, and showed very little scatter. The three films had J_n/J_c ratios of 0.54, 0.50 and 0.64, which is much less scatter than has been seen in previous 7° bicrystals, where the ratio varied from 0.35 to 0.95 [8].

The resistivity versus temperature curves for the intergrain and intragrain links on each of the three samples is plotted in Fig. 2. This data also show little scatter, and a comparison of the inter- and intragrain resistivity indicates that all the 7° grain boundaries clearly contribute to an additional normal state resistivity that is independent of thickness. Resistivity

versus temperature was also measured for the three CC links, and all the curves were quite similar. A representative curve is indicated in Fig. 2 by the squares. It shows that the CC samples have normal state resistivities that are close to those of single crystal films, despite consisting of many small misoriented grains with an average spread of 9° to 12° .

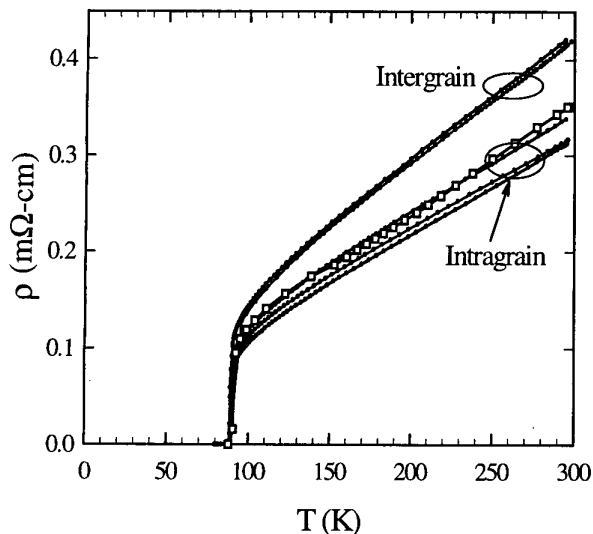


Fig. 2. Resistivity versus temperature for inter- and intragrain links on the 7° bicrystals. The square boxes indicate the coated conductor sample curve.

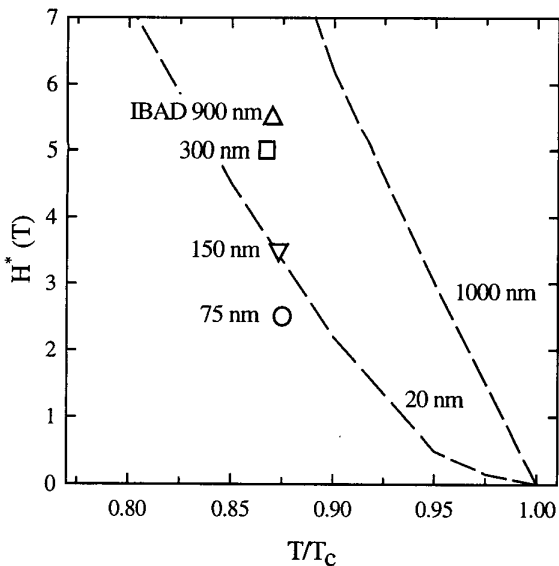


Fig. 3. The intragranular irreversibility field, H^* , measured at 77 K by transport measurements for different thickness films. The data are compared to ac susceptibility measurements of H^* on 20 nm and 1000 nm thick laser ablated $\text{YBa}_2\text{Cu}_3\text{O}_{7-x}$ films by Civale et al [10].

High sensitivity voltage-current characteristics of the bicrystals were taken in large magnetic fields at 77 K with the magnetic field parallel to the film c-axis. The irreversibility

field, H^* , is found experimentally by determining the magnetic field at which the E-J curve most closely approaches a power law expression. For the intragranular links on the bicrystal films and for the coated conductor samples, the results of these fits are summarized in Fig. 3. H^* is plotted versus reduced temperature, T/T_c , with the data at 77 K indicated by the symbols. The dashed lines show H^* measured by susceptibility for a 20 nm and a 1000 nm laser ablated film of $\text{YBa}_2\text{Cu}_3\text{O}_{7-x}$ by Civale et al. [10]. Both sets of data show a large increase in the irreversibility field with increasing thickness. Analysis of the intergrain E-J curves found that the presence of the 7° grain boundary did not change H^* or the observed thickness dependence. The susceptibility data in Fig. 3 defines H^* as the peak in the imaginary component, χ'' . The thickness dependence of H^* by transport occurs at lower magnetic fields than those seen by susceptibility, due to the ac nature of the susceptibility measurement, and the different criteria used to define H^* .

IV. MAGNETO-OPTIC AND SEM CHARACTERIZATION

Magneto-optic (MO) imaging and scanning electron microscopy were used to identify local defects in both the CC prototypes and the bicrystal films.

In Fig. 4, magneto-optic images of link A and B from the first CC sample are shown. The dark areas correspond to low magnetic fields, where the superconductor shielding currents are preventing the penetration of the applied 200 G field. There are obvious differences between the two images. Link A presents a very irregular profile, with many small defects that allow flux penetration, and also act as barriers to supercurrent flow. Link B is much more uniform, with no obvious "weak spots" that allow flux to penetrate.

MO images of link C and D were much the same as link B and A. However, along with many small regions of flux penetration, link D also had defects that extended across the link completely. Light and scanning electron microscopy found these large defects to be scratches in the YSZ substrate that were nucleation sites for very misaligned YBaCu_3O_x grains.

The CC samples were also studied by SEM, and some representative images are shown in Fig. 5. Fig. 5(a) shows link A, with the inset being a higher magnification image of the same link. Fig. 5(b) shows link B, again with an inset. All the links consist of submicron grains of $\text{YBa}_2\text{Cu}_3\text{O}_{7-x}$, along with numerous small lighter colored second phase particles. Observations on tilted samples showed that some $\text{YBa}_2\text{Cu}_3\text{O}_7$ colonies were misaligned with respect to the substrate, producing a rough surface. One feature is the large numbers of submicron voids seen in link A that are not seen in link B. This was also observed in link C and D, where link D had a much larger concentration of voids. These voids may contribute significantly to the lower J_c and greater granularity seen in link A and D, due to a shadowing effect that perturbs supercurrent flow [12].

V. DISCUSSION AND CONCLUSIONS

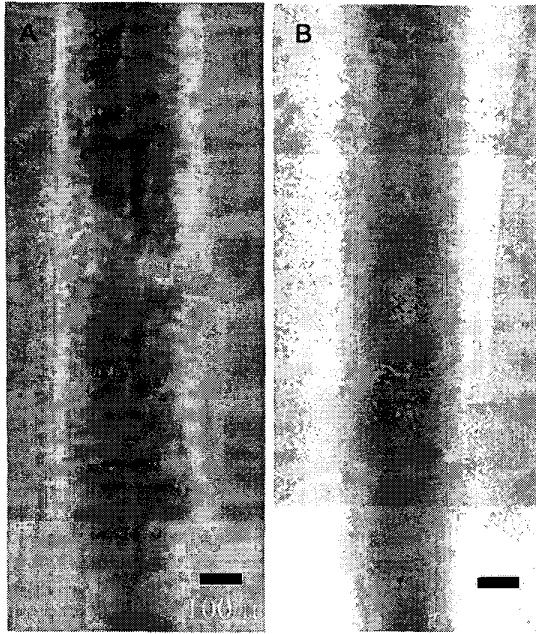


Fig. 4. Magneto-optic images of link A and B taken at 25 K and 200 Gauss after zero field cooling. Link A appears more granular while link B appears to be a homogeneous barrier to flux penetration.

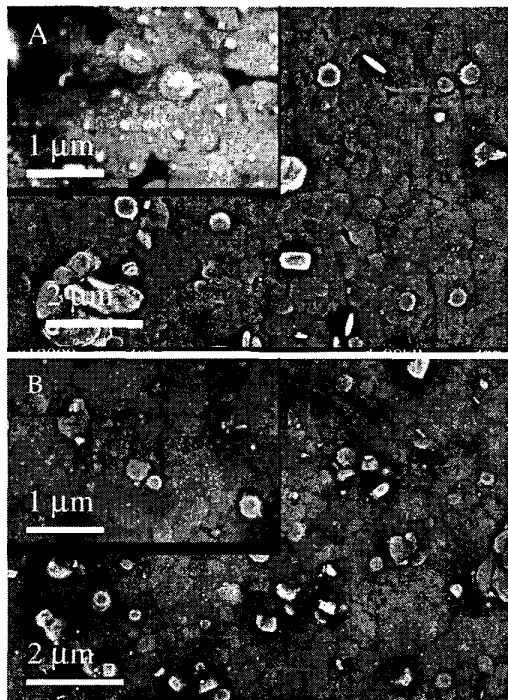


Fig. 5. SEM images of coated conductor prototypes. The top image is of link A, which has lower J_c , and the bottom image is of link B.

Coated conductor prototypes were studied and compared to epitaxially grown 7° low angle bicrystal films. Both types of material were studied by x-ray diffraction, transport, magneto-optic imaging, and SEM. Despite having large rocking curve FWHM values, the CC had resistivities and voltage-current characteristics almost identical to single crystal films with FWHM values of $< 1^\circ$. One reason may be that the growth conditions for CC are such that low angle grain boundaries do not act as weak links, as has been seen in earlier studies of some $7^\circ[001]$ thin film bicrystals [8].

Thickness dependence of the high field transport properties was also studied. The irreversibility field of both intra- and intergrain regions of the $7^\circ[001]$ bicrystals increased from 2.5 T at $0.075 \mu\text{m}$ thick to 5 T at $0.3 \mu\text{m}$ thick, which is consistent with the measured H^* of 5.5 T for the $0.9 \mu\text{m}$ thick CC samples.

The CC samples were also compared to one another. Despite macroscopically similar grain alignment, J_c values varied by almost a factor of two from link to link. Magneto-optic and SEM studies showed the presence of many small defects that were disrupting supercurrent flow in the lower J_c links. A likely cause for this disruption are the submicron sized voids seen in large numbers in the lower J_c links.

These studies indicate grain alignment with FWHM of 7° - 15° is sufficient for high J_c , strongly coupled behavior in coated conductor material, and further improvements will come by understanding and controlling other material defects such as scratches, voids, and second phase particles.

REFERENCES

- [1] Y. Iijima, K. Onabe, N. Futaki, N. Tanabe, N. Sadakata, O. Kohno, and Y. Ikeno, *J. Appl. Phys.*, vol. 74, p. 1905, 1993.
- [2] X.D. Wu, S.R. Foltyn, P.N. Arendt, W.R. Blumenthal, I.H. Campbell, J.D. Cotton, J.Y. Coulter, W.L. Hults, M.P. Maley, H.F. Safar, and J.L. Smith, *Appl. Phys. Lett.*, vol. 67, p. 2397, 1995.
- [3] A. Goyal, D.P. Norton, J.D. Budai, M. Paranthaman, E.D. Specht, D.M. Kroeger, D.K. Christen, Q. He, B. Saffian, F.A. List, D.F. Lee, P.M. Martin, C.E. Klabunde, E. Hartfield, and V.K. Sikka, *Appl. Phys. Lett.*, vol. 69, p. 1795, 1996.
- [4] D. Dimos, P. Chaudhari, and J. Mannhart, *Phys. Rev. B*, vol. 41, p. 4038, 1990.
- [5] T. Amrein, L. Schultz, B. Kabius, and K. Urban, *Phys. Rev. B*, vol. 51, p. 6792, 1995.
- [6] Z.G. Ivanov, P.Å. Nilsson, D. Winkler, J.A. Alarco, T. Claeson, E.A. Stepantsov, and A.Ya. Tzalenchuk, *Appl. Phys. Lett.* vol. 59, p. 3030, 1991.
- [7] N.F. Heinig, R.D. Redwing, I Fei Tsu, A. Gurevich, J.E. Nordman, S.E. Babcock, and D.C. Larbalestier, *Appl. Phys. Lett.* vol 69, p.577, 1996.
- [8] N.F. Heinig, R.D. Redwing, J.E. Nordman, and D.C. Larbalestier, submitted to *Phys. Rev. B*, 1998.
- [9] R.H. Koch, V. Foglietti, W.J. Gallagher, G. Koren, A.Gupta, and M.P.A. Fisher, *Phys. Rev. Lett.* vol. 63, p. 1511, 1989.
- [10] L. Civale, T.K. Worthington, and A. Gupta, *Phys. Rev. B*, vol. 43, p. 5425, 1991.
- [11] A. Sawa, H. Yamasaki, Y. Mawatari, H. Obara, M. Umeda, and S. Kosaka, *Phys. Rev. B*, vol. 58, pp. 2868-2877, 1998.
- [12] A. Gurevich, and J. McDonald, *Phys. Rev. Lett.*, to appear 1998.